

Carbon dioxide mediates Mn(II)-catalyzed decomposition of hydrogen peroxide and peroxidation reactions

Stefan I. Liochev and Irwin Fridovich*

Department of Biochemistry, Duke University Medical Center, Durham, NC 27710

Contributed by Irwin Fridovich, July 8, 2004

Mn(II) can catalyze the decomposition of H₂O₂ and, in the presence of H₂O₂, can catalyze the oxidation of NADH. Strikingly, these processes depend on the simultaneous presence of both CO₂ and HCO₃⁻. This explains the exponential dependence of the rates on [HCO₃⁻], previously noted by other workers. These processes are inhibited by Mn-superoxide dismutase, establishing the generation of O₂⁻ and its role as an essential reactant. A scheme of reactions, consistent with the known properties of this system, is proposed. The large rate enhancements provided by HCO₃⁻ + CO₂, and the abundance of both of these species *in vivo*, suggest that similar reactions have relevance to the oxidative stress imposed by O₂⁻ and H₂O₂.

The Cu,Zn superoxide dismutase (SOD1) catalyzes the oxidation of a variety of substrates by H₂O₂ (1–8). This peroxidative activity was thought to depend on HCO₃⁻ (2–7), but was shown to actually require CO₂ (8). Carbonate radical (CO₃⁻) is proposed to be the strong oxidant that is responsible for the peroxidations observed (3–8). HCO₃⁻-dependent peroxidations and H₂O₂ decomposition, catalyzed by Mn(II) and Fe(II), have been reported (9–17). The possibility that, in these reactions, CO₂ rather than HCO₃⁻ might be required, needs to be considered. One puzzling aspect of the Mn(II) + HCO₃⁻-catalyzed peroxidations and H₂O₂ decompositions was the exponential dependence of rates on [HCO₃⁻] within a given range of [HCO₃⁻]. Thus, Sychev *et al.* (9, 10) reported dependence of the rate on more than the square of [HCO₃⁻], whereas the Stadtman group (13) reported a third-order dependence on [HCO₃⁻].

In what follows, we demonstrate a dependence on CO₂ and an apparent synergism between CO₂ and HCO₃⁻, which largely explains the reported exponential responses to [HCO₃⁻]. The abundance of CO₂ and HCO₃⁻ in biological systems and their role in the peroxidations catalyzed by SOD1 and metal cations, such as Mn(II), could have relevance to the oxidative stress experienced by aerobic organisms.

Materials and Methods

NaHCO₃, MnCl₂, sodium pyrophosphate, and H₂O₂ were from Mallinckrodt; Tris was from Merck; catalase was from Roche Molecular Biochemicals; human MnSOD was from Biotechnology General (Rehovot, Israel); and NADH was from Sigma. Reaction mixtures usually contained 10 mM H₂O₂, 0.1 mM MnCl₂, and 20 mM NaHCO₃ in 100 mM Tris buffer at pH 7.4 and room temperature (23°C). Reactions were followed spectrophotometrically, and in cases where the addition of reactants entailed sudden changes in absorbance, due either to dilution or the absorbance of the reagent added, such changes were corrected in the data shown. When absorbance changes with time were too rapid to record, they are shown as dashed lines as in Fig. 3. CO₂ was added as ice-cold water saturated with CO₂ gas.

Results

Absorption Spectra. Addition of the third component (H₂O₂ or MnCl₂, or NaHCO₃), to Tris-buffered solutions of the other

two, initiated the changes in absorption spectrum shown in Fig. 1. It should be noted that several buffering species were explored, including phosphate, cacodylate, and Hepes, but only Tris supported the changes observed. Fig. 1A shows that the most rapid (0–3 min) was an increase in absorbance in the range of 250–350 nm and a decrease at wavelengths <250 nm. At longer reaction times (0–20 min), absorbance appeared at ≈270 nm, whereas the absorbance <250 nm first decreased and then increased, as shown in Fig. 1B. At still longer times (Fig. 1C), the band at ≈270 nm became more pronounced, a shoulder developed at ≈300 nm, and absorbance <250 nm decreased.

The species responsible for the absorbance centered at 270 nm is some stable product of Tris oxidation, as similar absorbance is seen in Tris buffer that has aged for many months. The kinetics of the absorbance change at 270 nm is shown in Fig. 2. Starting the reaction by adding NaHCO₃ caused a small but rapid increase at 270 nm, which was followed by a slower increase that was not interrupted by late addition of 48 μg/ml MnSOD, 0.5 mM pyrophosphate, or 120 units/ml catalase, any of which inhibited if present at the outset. The initial rapid increase at 270 nm was due to the rapidly formed species absorbing in the 250- to 350-nm region. Evidently, the stable A₂₇₀ species is produced from a preformed precursor and does not depend on the continued presence of H₂O₂, O₂⁻, or Mn(III). The latter deduction is based on the abilities of catalase to remove H₂O₂, MnSOD to remove O₂⁻, and pyrophosphate to complex and thus trap Mn(III).

The time course of the broad band followed at ≈300 nm is illustrated in Fig. 3. Addition of NaHCO₃ to the buffered solution of Mn(II) + H₂O₂ caused a rapid increase in absorbance that approached a plateau. This plateau evidently represented a dynamic steady state, as adding MnSOD (Fig. 3, line 1) or pyrophosphate (Fig. 3, line 2) caused a swift decline. The species followed at 300 nm could not have been Mn(III), because H₂O₂ was seen to instantly bleach the absorbance of Mn(III) acetate. These results indicate that both O₂⁻ and higher valent states of Mn(II) are needed for the formation of the A₃₀₀ species. The rate of appearance of the A₃₀₀ species was slower when NaHCO₃ was the last component added than it was when H₂O₂ was added last (Fig. 3). This could be explained by the relative slowness of the formation of CO₂ after the addition of the alkaline NaHCO₃ to the reaction mixture buffered at pH 7.4. This view is supported by the fact that carbonic anhydrase at 50 μg/ml, when present in the reaction mixture, sharply increased the rate seen when NaHCO₃ was added last and made it indistinguishable from line 2 in Fig. 3.

CO₂ Is a Reactant. The addition of NaHCO₃ initiated a rapid increase in A₃₀₀ that approached a plateau within 3 min, as seen

Abbreviation: SOD, superoxide dismutase.

*To whom correspondence should be addressed. E-mail: fridovich@biochem.duke.edu.

© 2004 by The National Academy of Sciences of the USA

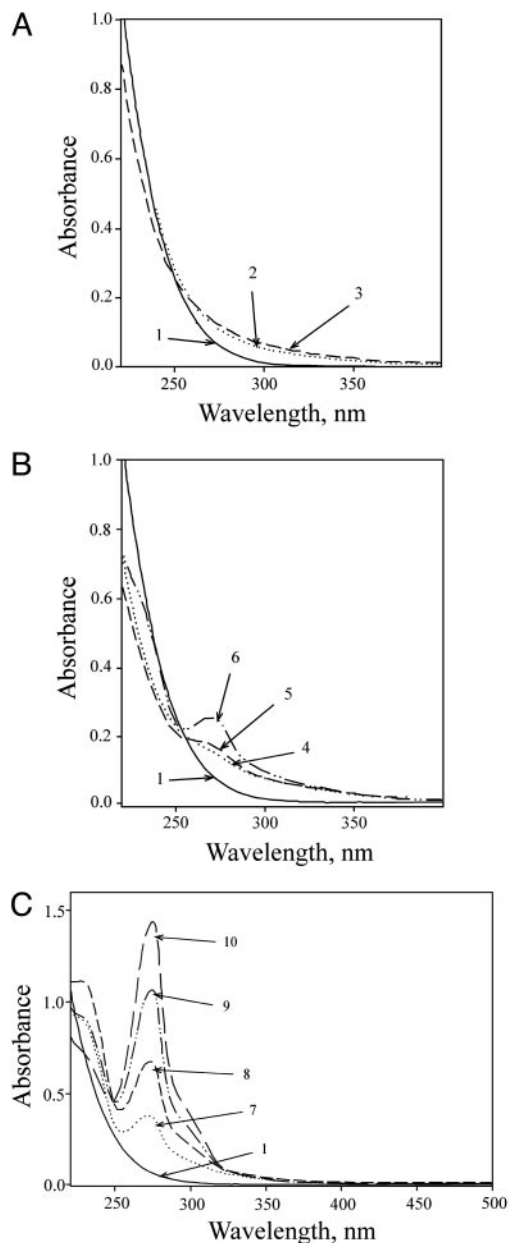


Fig. 1. Absorption spectra during the $\text{Mn} + \text{H}_2\text{O}_2 + \text{HCO}_3^-$ reaction. Reactions were started by adding NaHCO_3 to 20 mM to 10 mM H_2O_2 , 0.1 mM MnCl_2 , and 100 mM Tris chloride at pH 7.4. (A) Spectra taken at 0, 1, and 3 min (lines 1, 2, and 3). (B) Spectra taken at 0, 6, 10, and 20 min (lines 1, 4, 5, and 6). (C) Spectra taken at 0, 30, 50, 80, and 120 min (lines 1, 7, 8, 9, and 10). The zero time spectrum was taken before the addition of HCO_3^- .

in Fig. 3. When CO_2 was added, it caused a marked increase followed by a decline to the plateau that would have been reached in the absence of the addition of CO_2 , as seen in Fig. 4A. MnSOD (24 $\mu\text{g}/\text{ml}$) or pyrophosphate (0.5 mM) present at the outset prevented the increase in A_{300} (data not shown). The effect of added CO_2 was even more striking when the amount of HCO_3^- used to start the reaction was halved. Thus, as shown in Fig. 4B, the increase in A_{300} was decreased by ≈ 5 -fold when $[\text{HCO}_3^-]$ was halved, in agreement with an exponential dependence of rate on $[\text{HCO}_3^-]$. Subsequent addition of CO_2 again caused an abrupt but temporary increase in A_{300} (Fig. 4B, line 1). The presence of carbonic anhydrase eliminated the effect of added CO_2 (Fig. 4B, line 2). When CO_2 was added before, rather

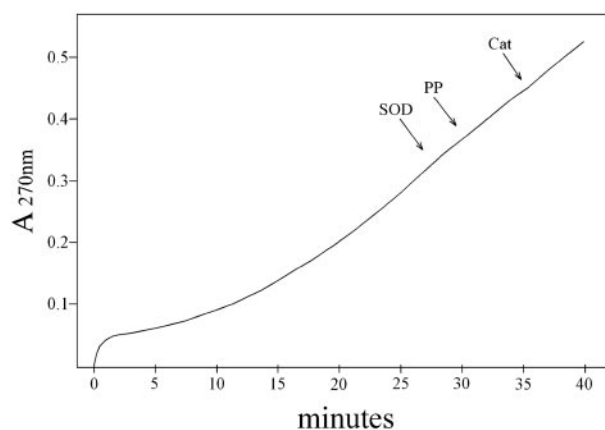


Fig. 2. Time dependence of absorbance at 270 nm. Reaction mixtures were as in Fig. 1, with the reaction started by the addition of HCO_3^- . At the arrows, MnSOD to 48 $\mu\text{g}/\text{ml}$, pyrophosphate (PP) to 0.5 mM, or catalase (Cat) to 120 units/ml was added.

than after, HCO_3^- , a very small and transient increase in A_{300} was seen, and the subsequent addition of HCO_3^- gave the modest and limiting increase in A_{300} that would have been observed in the absence of the CO_2 addition (Fig. 4B, line 3). Evidently, CO_2 greatly increases A_{300} only when HCO_3^- is also present. Clearly, CO_2 and HCO_3^- both are needed to support the reaction and behave synergistically.

The apparent difference between the effects of MnSOD and pyrophosphate, when added after the reaction was underway, as compared to their effects when added at the outset, is easily explained. Thus, there is overlap between the spectra of the A_{270} and A_{300} species. Thus, by the time the MnSOD or pyrophosphate had been added (Fig. 3), some of the stable A_{270} product had accumulated, and its absorbance at 300 nm prevented the complete ablation of the A_{300} . In contrast, when MnSOD or pyrophosphate was present at the outset, they prevented production of both the A_{300} and A_{270} species.

It thus appears that the rapidly forming A_{300} species is needed for production of the A_{270} species.

Consumption of H_2O_2 . Absorbance at 240 nm reflects both H_2O_2 and the rapidly forming A_{300} species. Hence, the reaction between Mn(II), H_2O_2 , HCO_3^- , and CO_2 produces a transient increase at 240 nm followed by a linear decrease (Fig. 5). Starting the reaction by adding NaHCO_3 last gave a slower increase in A_{240} than did adding MnCl_2 last (Fig. 5, compare lines 1 and 2).

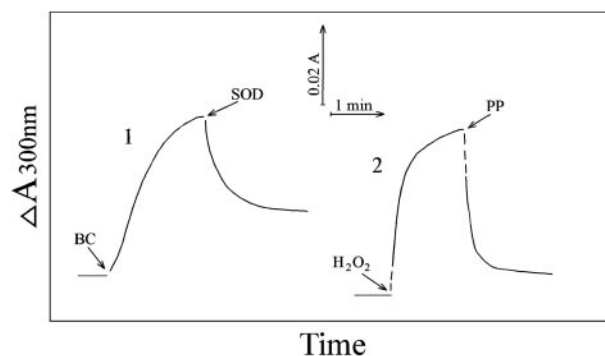


Fig. 3. Time dependence of absorbance at 300 nm. Reaction conditions were as in Fig. 1. Line 1, HCO_3^- (BC) added at the first arrow and MnSOD to 24 $\mu\text{g}/\text{ml}$ at the second arrow. Line 2, H_2O_2 added at the first arrow and pyrophosphate (PP) to 0.5 mM at the second arrow.

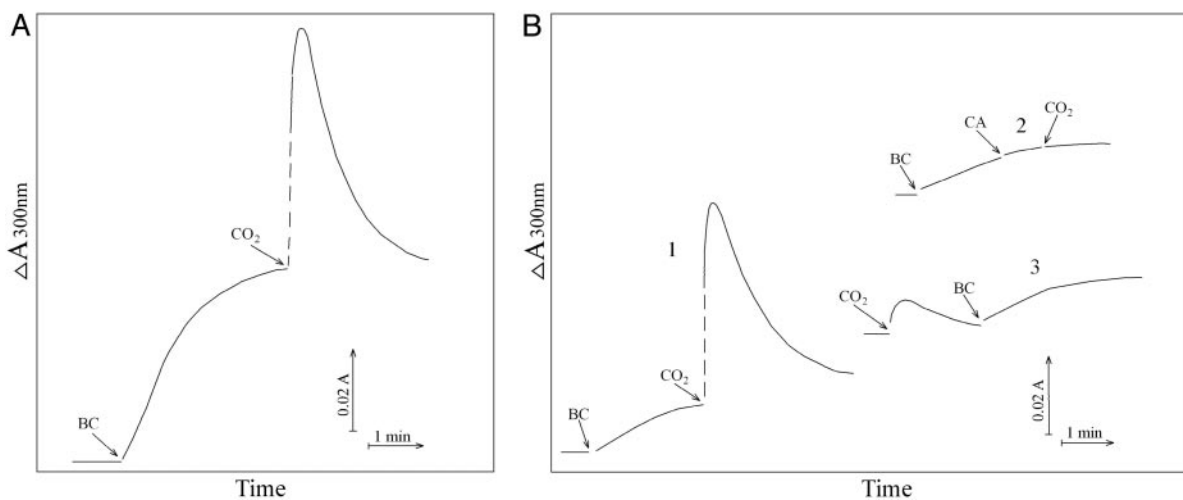


Fig. 4. Effect of CO₂ on absorbance at 300 nm. (A) Conditions were as in Fig. 1. Reaction was started by addition of HCO₃⁻ at the first arrow and 0.15 ml of ice water saturated with CO₂ added to the total volume of 3.0 ml at the second arrow. (B) Conditions were as in Fig. 1 except that HCO₃⁻ was added to 10 mM. Line 1, HCO₃⁻ added at the first arrow. Line 2, carbonic anhydrase (CA) was added to 50 μg/ml at the second arrow and CO₂ added at the third arrow. Line 3, CO₂ added at the first arrow and HCO₃⁻ added at the second arrow.

This is explained by the slowness of the uncatalyzed dehydration of H₂CO₃ to CO₂, as shown by the effect of carbonic anhydrase (Fig. 5, line 3). The linear decrease in A₂₄₀ that followed the transient increase reflects consumption of H₂O₂, which was ≈0.5 mM/min, of H₂O₂, and it was not influenced by carbonic anhydrase (Fig. 5, compare lines 1 and 3). Ethanol at 1% did not inhibit, but MnSOD or pyrophosphate did when added after the linear rate had been achieved, after a lag of 5–10 s (data not shown).

Addition of CO₂ increased the consumption of H₂O₂ as illustrated by line 1 in Fig. 6A. Prior addition of carbonic anhydrase eliminated this effect of CO₂, as shown by Fig. 6A, line 2. The effect of CO₂ was even more striking when the concentration of HCO₃⁻ was decreased from 20 to 10 mM. Thus, as shown in Fig. 6B, the rate of H₂O₂ consumption was then much slower, ≈0.1 mM/min, and the effect of added CO₂ was more obvious. The presence of carbonic anhydrase eliminated the effect of added CO₂, as shown by Fig. 6A, line 2. CO₂ was able to enhance the rate of H₂O₂ decomposition only if HCO₃⁻ was present. Thus, as shown by line 1 in Fig. 6C, addition of CO₂ to the Tris-buffered mixture of Mn(II) plus H₂O₂ was without

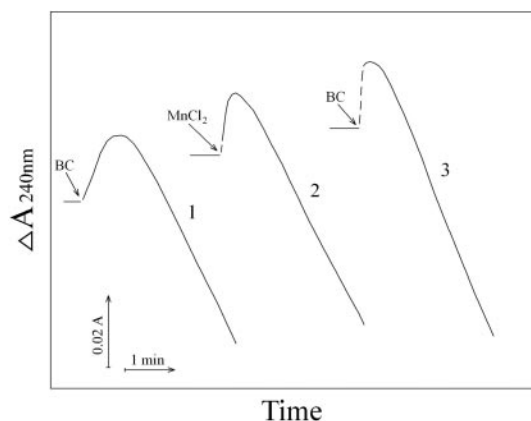


Fig. 5. Kinetics of absorbance changes at 240 nm. Conditions were as in Fig. 1. Line 1, reaction was started by the addition of HCO₃⁻. Line 2, reaction was started by the addition of Mn(II). Line 3, carbonic anhydrase was present at 50 μg/ml, and reaction was started by the addition of HCO₃⁻.

effect, and subsequent additions of 10 mM HCO₃⁻ gave the rates previously seen at these levels of HCO₃⁻ in the absence of CO₂ addition. Doubling the amount of CO₂ added, in the absence of HCO₃⁻ (Fig. 6C, line 2), had only a small effect, undoubtedly due to some conversion to HCO₃⁻. These results again bespeak a synergism between CO₂ and HCO₃⁻, due to the requirement for both to support the decomposition of H₂O₂.

Oxidation of NADH. Previous workers (11, 12, 14, 17) demonstrated that Mn(II) + H₂O₂ + HCO₃⁻ could cause the oxidation of diverse substrates, such as amino acids. We chose NADH because it absorbs at 340 nm, where the rapidly formed A₃₀₀ species does not absorb significantly. Moreover, CO₃^{•-}, considered a likely oxidant in this reaction system, is known to oxidize NADH with a rate constant of ≈10⁹ M⁻¹·s⁻¹ at 25°C (18). It should also be noted that HO• attacks NADH at sites that do not yield NAD⁺, whereas CO₃^{•-} does so (18). Line 1 in Fig. 7A shows that addition of HCO₃⁻ to 20 mM to the Tris-buffered mixture of H₂O₂ + Mn(II) initiated oxidation of NADH at a rate of ≈0.02 mM/min after a brief lag. Halving the amount of HCO₃⁻ added decreased the rate by 5.3-fold, and subsequent addition of CO₂ greatly increased the rate (Fig. 7A, line 2). MnSOD inhibited the oxidation of NADH, and this inhibition was not overcome by subsequent addition of CO₂ (Fig. 7A, line 3). The lags seen when HCO₃⁻ was used to start the reaction were not as evident when Mn(II) or H₂O₂ was the last component added, or when carbonic anhydrase was present at the time HCO₃⁻ was added (Fig. 7B). It follows that the lags seen in Fig. 7A were due to the time required for conversion of some of the HCO₃⁻ to CO₂. Ethanol added to 1% did not inhibit NADH oxidation (Fig. 7B, line 1), whereas MnSOD did so (Fig. 7B, line 2). Thus, HO• is not an intermediate in this process, but O₂⁻ is. In full accord with the deductions so far, adding CO₂ after HCO₃⁻ caused a marked increase in the rate of NADH oxidation (Fig. 7C, line 1), and this effect of CO₂ was eliminated if carbonic anhydrase was present (Fig. 7C, line 2). Addition of CO₂ in the absence of HCO₃⁻ transiently increased the rate due undoubtedly to the generation of some HCO₃⁻, the second component needed.

Discussion

One aspect of the toxicity of O₂⁻ is thought to involve the univalent oxidation of the [4Fe–4S] clusters of dehydrases,

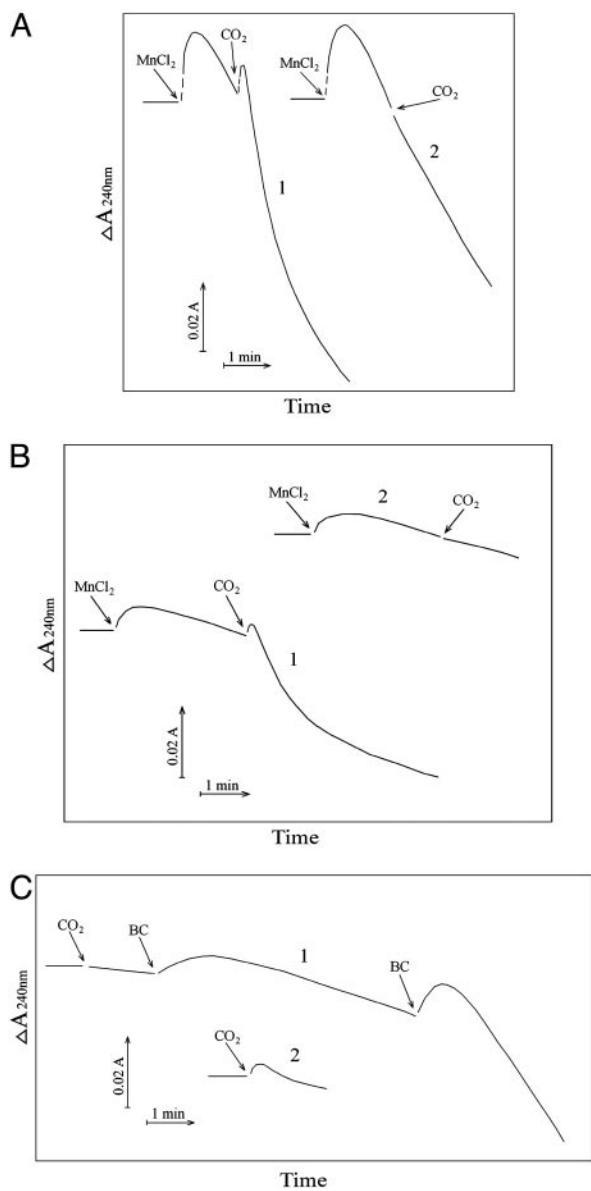


Fig. 6. Effects of CO_2 on absorbance changes at 240 nm. (A) Conditions were as in Fig. 1. Line 1, reaction was started by addition of Mn(II) at the first arrow, and then CO_2 was added at the second arrow. Line 2 was as in line 1, but carbonic anhydrase was present at $50 \mu\text{g/ml}$. (B) Conditions were as in A except that HCO_3^- was present at 10 mM . (C) Line 1, CO_2 was added to Tris-buffered solution containing $10 \text{ mM H}_2\text{O}_2$ and 0.1 mM Mn(II) at the first arrow, and then HCO_3^- to 10 mM was added at the second arrow, and at the third arrow HCO_3^- was raised to 20 mM . Line 2, 0.3 ml of CO_2 solution was added to the $\text{H}_2\text{O}_2 + \text{Mn(II)}$ reaction mixture at the arrow.

such as aconitase. This destabilizes the clusters causing release of Fe(II) , and that released iron can then generate potent oxidants by reacting with hydroperoxides, in what is called Fenton chemistry (19). Iron is not the only metal cation that can participate in Fenton chemistry. Thus, Mn(II) , Co(II) , Cr(II) , and Cu(II) can do likewise, and HCO_3^- or CO_2 has been shown to enhance the oxidations caused by several of these metals in the presence of H_2O_2 (11, 12, 14, 16, 20). In one of these cases, Xiao *et al.* (20) showed that CO_2 enhanced the luminescence of luminol caused by $\text{Co(II)} + \text{H}_2\text{O}_2$. H_2O_2 decomposition and oxidations, catalyzed by $\text{Mn(II)} + \text{H}_2\text{O}_2$, in the presence of HCO_3^- , have been studied by a number of

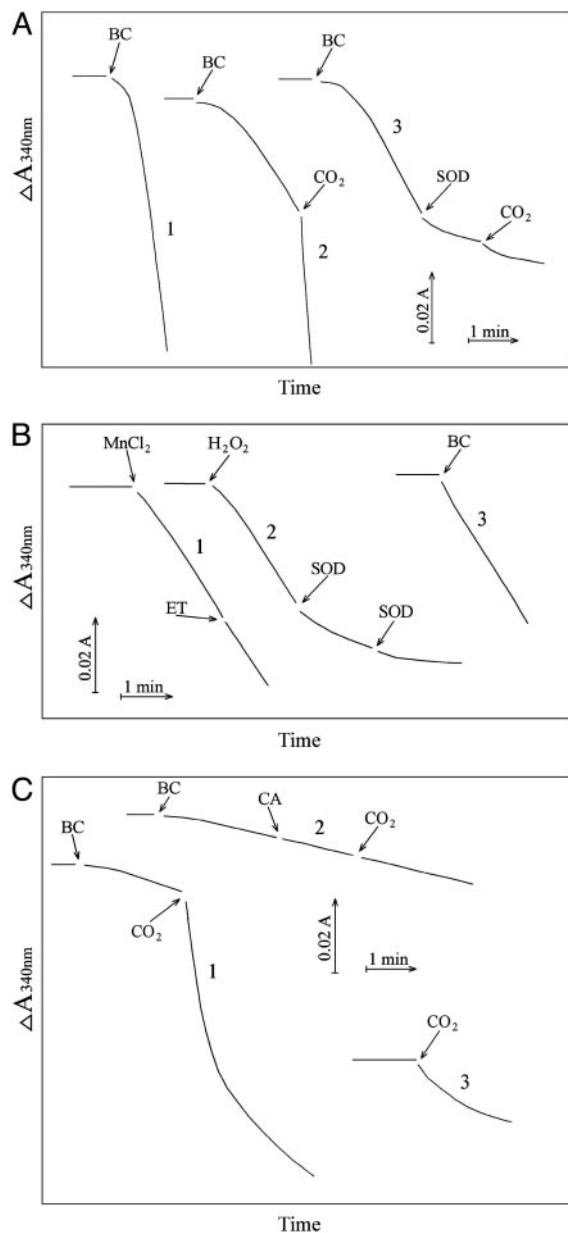
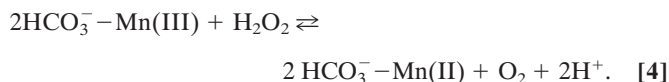
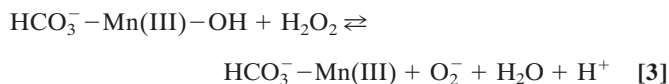
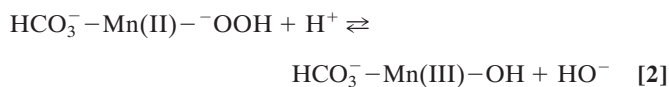
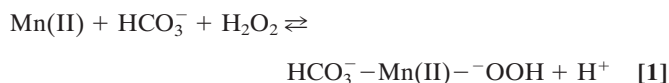


Fig. 7. Oxidation of NADH. NADH was present at 0.1 mM , and oxidation was followed at 340 nm . (A) Line 1, conditions were as in Fig. 1 except as noted below, and HCO_3^- was added to 20 mM at the arrow. Line 2, HCO_3^- was added to 10 mM at the first arrow, and 0.15 ml of CO_2 solution was added at the second arrow. Line 3, HCO_3^- was added to 10 mM at the first arrow, MnSOD was added to $30 \mu\text{g/ml}$ at the second arrow, and 0.15 ml of CO_2 solution was added at the third arrow. (B) Mn(II) was added at 0.1 mM , H_2O_2 was added at 10 mM , and HCO_3^- was added at 10 mM . Line 1, Mn(II) was added at the first arrow, and ethanol to 1% was added at the second arrow. Line 2, reaction was started with H_2O_2 at the first arrow, and then MnSOD was added to $6 \mu\text{g/ml}$ at the second arrow and to $18 \mu\text{g/ml}$ at the third arrow. Line 3, as in lines 2 and 3 in A but carbonic anhydrase was present at $50 \mu\text{g/ml}$. (C) Mn(II) was added at 0.1 mM , H_2O_2 at 10 mM , and HCO_3^- , when present, at 5 mM . Line 1, HCO_3^- was added at the first arrow, and 0.15 ml of CO_2 solution was added at the second arrow. Line 2, HCO_3^- was added at the first arrow, carbonic anhydrase to $50 \mu\text{g/ml}$ was added at the second arrow, and 0.15 ml of CO_2 solution was added at the third arrow. Line 3, 0.15 ml of CO_2 solution was added at the arrow, but HCO_3^- was not present.

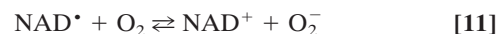
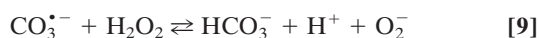
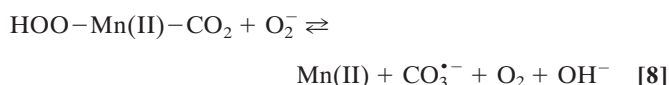
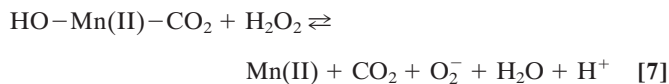
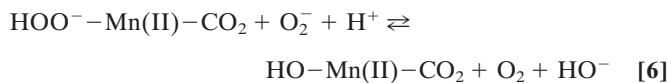
workers, such as Sychev *et al.* (9–12) and the Stadtman group (13–15); the exponential dependence of rate on $[\text{HCO}_3^-]$ has been noted, and mechanisms have been proposed.

Our present demonstration that both HCO_3^- and CO_2 are required for this process explains the exponential dependence on $[\text{HCO}_3^-]$, as elevating $[\text{HCO}_3^-]$ also raises the $[\text{CO}_2]$ in equilibrium with it. Any valid mechanism must explain the dual requirement for HCO_3^- and CO_2 and also the involvement of O_2^- . Moreover, analogy with the $\text{Cu,ZnSOD} + \text{H}_2\text{O}_2$ system indicates that $\text{CO}_3^{\bullet-}$ is a likely participant, whereas HO^\bullet is not (1, 3–8). The role of O_2^- could not be the reduction of Mn(III) to Mn(II), as suggested by the Stadtman group (13), because H_2O_2 itself rapidly accomplishes this reduction. On the other hand, the oxidation of Mn(II) to Mn(III) is also not likely to be the role of O_2^- , as H_2O_2 would then be produced from the O_2^- , yet rapid H_2O_2 consumption is a hallmark of this process.

The following scheme of reactions is in accord with the known properties of the system. It is proposed in the realization that it is an oversimplification that others may want to elaborate.



In reactions 1–4, H_2O_2 has been decomposed to $\text{H}_2\text{O} + \text{O}_2$, and O_2^- has been generated, in what may be viewed as the initiation phase, setting the stage for the chain reaction depicted by the following reactions. In what follows, the manganese may or may not be participating in the form of an HCO_3^- complex.



The O_2^- generated in reaction 3 is essential for reactions 6 and 8, and it may be viewed as the initiating radical. This is in accord with the observation by Sychev *et al.* (10) that tetranitromethane, which reacts with O_2^- at $\approx 10^9 \text{ M}^{-1}\text{s}^{-1}$, strongly inhibited the decomposition of H_2O_2 and that the simultaneous addition of tetranitromethane and *N,N'*-dimethyl-*p*-nitrosoaniline prevented the oxidation of the *N,N'*-dimethyl-*p*-nitrosoaniline until all of the tetranitromethane was consumed. In our case, we used MnSOD, which scavenges O_2^- as efficiently as does tetranitromethane, but which acts catalytically rather than stoichiometrically. The product of reaction 6 may itself act as the oxidizing species, or carbonate radical, made as in reaction 8, may be the oxidant that can oxidize H_2O_2 (reaction 9) or NADH (reaction 10). Reactions 6 and 7 or 8 and 9 may be alternative or simultaneous pathways. Note the similarity of pathways 6 and 7 as well as 8 and 9 to the classical Haber–Weiss chemistry (21). Because O_2^- is merely acting as a reductant, other reductants in the cell could possibly trigger these potentially damaging processes. Reaction 12 is a termination reaction, and it explains the inhibition by MnSOD. The product of reaction 2 contains trivalent manganese, and it could be the site of inhibition by pyrophosphate. Oxidation of Tris by one or more of the oxidants generated in this scheme would account for the slowly forming and stable species followed at 270 nm. Sychev *et al.* (9, 10) worked without buffer and maintained pH by titration. Hence, it cannot be the case that Tris is needed for the process under study. We must rather conclude that Tris did not significantly interfere whereas phosphate, Hepes, and cacodylate did so.

The biological significance of Fenton chemistry has been questioned in part because the rate constants for the reactions of reduced metals, and their complexes, with H_2O_2 are not rapid, and their *in vivo* metal ligands are unknown (22). The present observations of the synergistic rate accelerations by $\text{HCO}_3^- + \text{CO}_2$ plus the work of Sychev *et al.* (9–12) and the Stadtman group (13–16) overcome this bottleneck and may well be of importance in the imposition of oxidative stress in biological systems. In this regard, the observation of Stadtman and Berlett (16) that HCO_3^- greatly enhances the ability of Fe(II) plus H_2O_2 to cause the oxidation of amino acids is also very interesting. The exponential dependence of rates on $[\text{HCO}_3^-]$ can have two components. Thus, the second-order dependence reported by Sychev *et al.* (10) is explained by the dual need for HCO_3^- and CO_2 . To this can be added the effect of HCO_3^- in decreasing the amount of free hexaquo Mn(II) available for consumption of O_2^- by the reaction $\text{Mn(II)} + \text{O}_2^- + 2\text{H}^+ \rightleftharpoons \text{Mn(III)} + \text{H}_2\text{O}_2$. This, together with the need for $\text{CO}_2 + \text{HCO}_3^-$, could explain the third-order dependence noted by the Stadtman group (13).

This work was supported by National Institutes of Health Grant DK5986A.

- Hodgson, E. K. & Fridovich, I. (1975) *Biochemistry* **14**, 5299–5303.
- Sankarapandi, S. & Zweier, J. L. (1999) *J. Biol. Chem.* **274**, 1226–1232.
- Liochev, S. I. & Fridovich, I. (1999) *Free Radical Biol. Med.* **27**, 1444–1447.
- Zhang, H., Joseph, J., Felix, C. & Kalyanaraman, B. (2000) *J. Biol. Chem.* **275**, 14038–14045.
- Zhang, H., Joseph, J., Gurney, M., Becker, D. & Kalyanaraman, B. (2002) *J. Biol. Chem.* **277**, 1013–1020.
- Zhang, H., Andrekopoulou, C., Joseph, J., Chandran, K., Karoui, H., Crow, J. P. & Kalyanaraman, B. (2003) *J. Biol. Chem.* **278**, 24078–24089.
- Liochev, S. I. & Fridovich, I. (2002) *J. Biol. Chem.* **277**, 34674–34678.
- Liochev, S. I. & Fridovich, I. (2004) *Proc. Natl. Acad. Sci. USA* **101**, 743–744.

- Sychev, A. Y., Isak, V. G. & Lap, D. V. (1977) *Russ. J. Phys. Chem.* **51**, 212–214.
- Sychev, A. Y., Isak, V. G. & Lap, D. V. (1978) *Russ. J. Phys. Chem.* **52**, 55–59.
- Sychev, A. Y., Phannmeller, U. & Isak, V. G. (1983) *Russ. J. Phys. Chem.* **57**, 1349–1351.
- Sychev, A. Y., Him, M. H. & Isak, V. G. (1984) *Russ. J. Phys. Chem.* **58**, 549–551.
- Stadtman, E. R., Berlett, B. S. & Chock, P. B. (1990) *Proc. Natl. Acad. Sci. USA* **87**, 384–388.
- Berlett, B. S., Chock, P. B., Yim, M. B. & Stadtman, E. R. (1990) *Proc. Natl. Acad. Sci. USA* **87**, 389–393.

